Modeling, Simulation and Kinetic Parameter Estimation in Batch Crystallization Processes

Robert J. Farrell and Yen-Cheng Tsai
Dept. of Chemical Engineering, Polytechnic University, Brooklyn, NY 11201

A dynamic model of a seeded batch crystallizer is used to investigate the process-dependent aspects of nucleation and growth kinetic parameter estimation by computer simulation. The satisfactory identification of all parameters in power-law-type kinetics with respect to supersaturation requires the use of nonlinear parameter transformations. The proper choice for transformation is problem-dependent, becoming more sensitive as nucleation rates increase, and the percentage of crystals below the measurable range increases.

Introduction

The onset of instability in industrial continuous crystallization processes in response to small disturbances has previously been shown to be determined primarily by the strong nonlinear dependence of nucleation rates on the relative supersaturation driving force (Buyevich et al., 1991; Jager et al., 1991). Consequently, accurate kinetic modeling of crystallization kinetics, especially nucleation, is a prerequisite to the optimal design and control of crystallization processes. Seeded batch experiments provide a convenient means of obtaining kinetic data, since batch runs permit investigations over wider ranges of supersaturations and are less time-consuming than MSMPR studies (Tavare and Garside, 1986). Using the batch data, nonlinear optimization can be used to fit kinetic parameters to the data (Eaton and Rawlings, 1990; Witkowsky et al., 1989; Stewart et al., 1992). As formulated using SimuSolv (Steiner et al., 1990), the procedure involves: (1) constructing a differential/algebraic process model for batch crystallization; (2) sequentially solving the model for parameter sets until a logarithmic likelihood objective function constructed from the measured response function and model-generated response and covariance is maximized. In practice, however, the identification of reaction rate models will present problems whenever limitations to the operating range of experimental apparatus do not permit the identification of a full mechanistic model (Box and Hill, 1967).

For limited sample sizes, reparameterizing the model in a close-to-linear form can improve results as well as speed convergence (Bates and Watts, 1981, 1988). Ratkowsky (1985) has discussed applications of reparameterization to solid-phase catalytic reactions. Recently, Edgar and Wright (1992) used reparameterization to obtain preexponential and activation energy parameters for the water gas shift reaction in a fixed-bed catalytic reactor using a data set involving a narrow temperature range. Chen and Aris (1992) also used reparameterization and rescaling to obtain Arrhenius parameters. For complex models, there is little guidance regarding the proper choice for the reparameterization function. Usually, it is necessary to experiment with several transformations (Bates and Watts, 1988). In fact, suitable reparameterizations for a particular process model may change for different data sets (Ratkowsky, 1983).

For batch crystallization, difficulties with CSD measurements below 4 micron can limit the information content of the data. The relative success of previous experimental studies may be explained by the relative importance of small particle measurements to the identification of a process model. Qui and Rasmunson (1991) have successfully identified nucleation and growth kinetics for succinic acid in a batch cooling crystallizer. This system is easily identifiable since it is characterized by low nucleation rates and high growth. On the other hand, Rawlings and coworkers have reported difficulties with a naphthalene-toluene system (Witkowski et al., 1989). In their study, CSD information derived from a light scattering (obscuration) measurement was combined with solute desupersaturation data. The obscuration measurement was related to the second moment of the CSD to solve the small particle-size measurement problem. Noise in the obscuration measurement, however, forced the use of a low weighing factor in the optimization routine. This effectively lowered the information

Correspondence concerning this article should be addressed to R. J. Farrell.

content of the data set resulting in poor confidence for the nucleation parameters.

The primary objective of this work is to examine the potential applications of reparameterizations to identify batch crystallization kinetics. We have chosen to use computer-generated data to permit the investigation of the technique as applied to extremes of growth and nucleation rates without introducing complications of experimental inaccuracies. For simplicity, the parameters studied here concern size-independent growth and secondary nucleation. The model, however, may be adapted for more complex parameters including agglomeration, breakage, primary nucleation, growth rate dispersion, and dispersion of initial nuclei-size distribution.

A secondary objective addresses the construction of a suitable differential/algebraic process model for crystallization. Witkowsky et al. (1989) used a collocation model; however, these are difficult to formulate since the choice of the orthogonal functions are arbitrary and problem-dependent (deWolf et al., 1990; Marchal et al., 1988). Here, the method of lines discretion (Hounslow et al., 1988) is used. Acceptable model accuracy is obtained by combining fixed ratio and fixed interval discretation along the size axis. Unlike previous discretation models, we introduce a variable time delay model for the nucleation boundary condition. The time delay formulation differs from previous models which insert nucleated particles into the smallest size class at birth, thereby potentially overpredicting desupersaturation rates. In addition, the new formulation permits the definition within the model of the percent of "uncounted crystals," that is, the percent of total crystals that have not grown to a measurable range. Successful parameter estimation is shown to depend increasingly on the proper choice of a reparameterization function as the percentage of uncounted crystals increases.

Mathematical Model

Problem definition

Consider the batch nonisothermal crystallization process described by:

$$N=f(N,T,c,d,p,t) \tag{1}$$

$$c=f(N,T,c,d,p,t) \tag{2}$$

where N is the dependent output variable vector representing the number of crystals in a specific size increment, and c generically represents the solution species concentration, a dependent output variable. T represents the known batch temperature profile, d unknown inputs, p process parameters, and t time.

The crystal population balance can be approximated as a set of ordinary differential equations by discretization along the size axis. For example, for size-independent growth processes, which assume a constant crystallizer volume without agglomeration or breakage, the first-order method of lines scheme (Kramer et al., 1990) utilizing a geometric grid ($r=L_{i+1}/L_i$) reduces to (Hounslow et al.,1988):

$$\frac{dN_i}{dt}=\frac{G}{L_i(r-1)}\left[rN_{i-1}-N_i+B_i\right] \tag{3}$$

where nucleation is assumed to occur only at the smallest L ($B_i=0$ for $i\neq 1$). The initial seed distribution, N_0 and solution concentration c_0 are known, so that the solution species concentration can be computed algebraically from the magma density, that is, the third moment of the discretized population balance, by material balance:

$$c=f(N_0,c_0,MT) \tag{4}$$

Growth and secondary nucleation rates are computed from a power law relationship to the relative supersaturation according to:

$$G=k_g\Delta c^g \tag{5}$$

$$B_0=k_b\Delta c^b MT^j \tag{6}$$

where the supersaturation Δc is found from Eq. 4 and a known temperature-dependent solubility relationship. Usually it is assumed that $B_1=B_0$; for this study, B_1 is computed using the time-delayed formulation of Eq. 14.

Assuming $j=1$, the kinetic parameters to be identified are k_g, g, k_b, and b. Defining a measurement vector y, the parameter estimation problem is written as a nonlinear optimization problem (NLP). For the objective function, SimuSolv maximizes a log likelihood objective function.

$$\text{maximize } \Phi(\bar{p},y,\bar{y}) \tag{7}$$

where

$$\bar{y}=f(\bar{N},\bar{t}) \tag{8}$$

Discretation accuracy

A convenient measure of discretation accuracy is obtained by comparing the analytic solution for the moment transients for isothermal size-independent growth (Randolph and Larson, 1988) vs. discrete model predictions. Summing over all discrete sizes, the jth moment (m_j) is given by:

$$m_j=\sum_i (\overline{L_i^j})N_i \tag{9}$$

where the proper mean for each moment is (Hounslow et al., 1988):

$$\overline{L_i^j}=\frac{1}{j+1}\left(\frac{r^{j+1}-1}{r-1}\right)L_i^j \tag{10}$$

Substituting and differentiating for the rate of change of moments:

$$\frac{dm_j}{dt}=jGm_{j-1}\left[\frac{1}{j+1}\frac{r^{j+1}-1}{r-1}\right] \tag{11}$$

The bracketed term arises due to discretation. It represents an overprediction in comparison to the analytic solution resulting from the geometric discretization. For $r=\sqrt[3]{2}$, this error is 13,

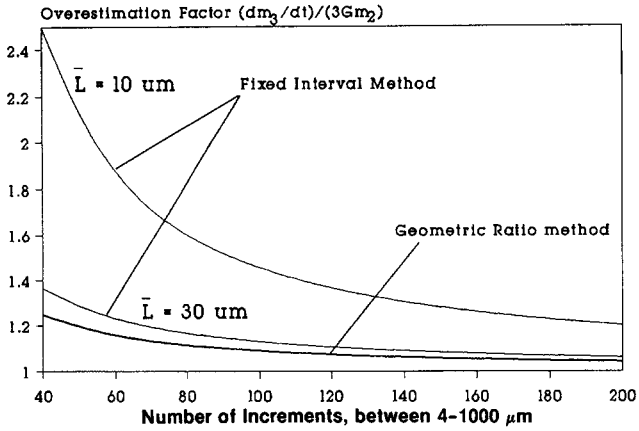

Figure 1. Overestimation factor for third moment.

28 and 45% for the first, second and third moments. Errors in the third moment are reflected in the kinetic parameters since the solution species concentration is computed from Eq. 4 and thereby influence the parameters in Eqs. 5 and 6.

Alternately, Eq. 3 may be formulated using fixed interval discretization: $(\mathcal{L}_{i+1} = \mathcal{L}_1 + (i)\Delta\mathcal{L})$. For equal increments, fixed interval discretation allows more states at the higher sizes, which is desirable for seeded processes, since the CSD is bimodal. The rate of change of moments is now (Appendix A):

$$\frac{dm_j}{dt} = jGm_{j-1} \cdot \left[\frac{1}{j(j+1)} \sum_{k=1}^{j} \binom{j+1}{k} \Delta\mathcal{L}^{k-1} \times (j+1-k) \frac{m_{j-k}}{m_{j-1}} \right] \quad (12)$$

Because of the appearance of the particle moment ratios in the brackets, the fixed interval overestimation factor is not only a function of the increment size but also the system CSD. Equation 12 will predict a smaller error for higher system mean sizes.

Figure 1 compares the overestimation factor for the third moment for geometric and fixed discretation per Eqs. 11 and 12. Obviously, discretation error is reduced by increasing the number of model increments. Note that for a fixed number of size classes, geometric discretation is superior, especially when compared at smaller system mean sizes. A fixed interval scheme, however, will increase the number of intervals in the higher size classes allowing a closer fit to experimental data. A mixed discretation scheme, utilizing fixed ratio for small sizes and fixed interval for larger sizes is therefore a good choice when run time and CPU considerations require a minimal number of state equations.

In an alternate model formulation, Hounslow et al. (1988) minimized discretation error by redefining discretized growth as:

$$\frac{dN_i}{dt} = \frac{G}{L_i} [aN_{i-1} + bN_i + cN_{i+1}] \quad (13)$$

For $r = \sqrt[3]{2}$, the authors computed values of a, b, and c that reduced the overprediction for the third moment to 1.8%. Recently, Hostomsky and Jones (1991) proved this approach to be flawed in that the net sum of the growth contributions of the individual classes will result in nonvanishing terms on the righthand side, thereby altering the apparent nucleation predictions of the model. They modified the growth expression in the first class to insure that all terms on the righthand side of Eq. 13 vanish. For the first-order method of lines approach used in this study, all righthand side terms vanish.

Nucleation boundary condition

As a consequence of defining the birth of nuclei at a finite size $(B_1 = B_0)$, an error is introduced in the calculated model solution species concentrations (Eq. 4), which overpredicts desupersaturation. For the first increment, an alternate formulation for the number of particles due to nucleation in terms of the zero-size nucleation rate is proposed as:

$$B_1 = B_0 \mu(t - \tau_D) \quad (14)$$

where $\mu(t-\tau_d)$ represents a unit step function, and τ_D represents a variable time delay. The time delay represents the time for nuclei to grow from birth to the first model increment. For batch crystallization, τ_D increases with batch time since growth rate falls. More details regarding the implementation of Eq. 14 are given in Appendix B.

Defining the first model class as the smallest measurable crystal size permits the definition of a term representing the percentage "uncounted" crystals that have been born, but not grown to the first increment:

$$\%\,Unc = \frac{(\Sigma N_i)_{t=0} + \int_0^t B_0 dt' - (\Sigma N_i)_{t=t}}{\int_0^t B_0 dt' + (\Sigma N_i)_{t=0}} \times 100 \quad (15)$$

For parameter estimation, Eq. 15 may be considered as a quantitative measure of the information content of the CSD data. The percentage uncounted crystals also reflects the relative importance of the time-delayed nucleation formulation. Higher overprediction of desupersaturation rates will occur for processes having higher uncounted crystals.

Model stability considerations

Using the Euler algorithm with integration step size Δt,

$$N(i)_{t+1} = N(i)_t + (dN(i)/dt)_t \, \Delta t \quad (16)$$

Substituting Eq. 3 and expanding (ignoring nucleation),

$$N(i)_{t+1} = N(i)_t + \frac{G\Delta t}{L_i - L_{i-1}} N_{i-1} - \frac{G\Delta t}{L_{i+1} - L_i} N_i \quad (17)$$

The term $G\Delta t/(L_{i+1} - L_i)$ represents the fraction of N_i that grows out of the size interval in time step Δt. As a conservative criteria for stability, Δt should be chosen to insure that this fraction does not exceed unity. If the integration step size is too large, oscillations and negative values in the N_i vector may

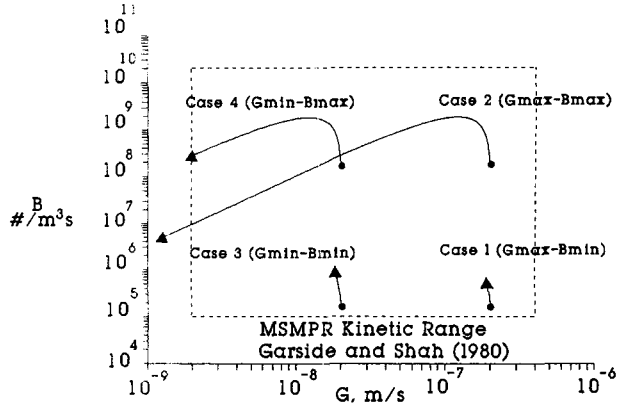

Figure 2. Range of growth and nucleation rates.

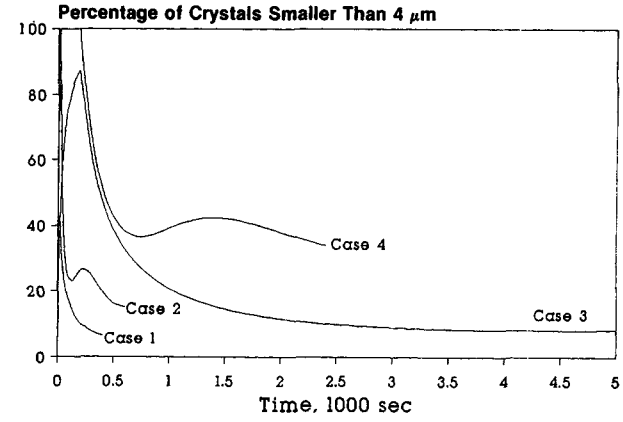

Figure 3. Uncounted crystals (Eq. 15) vs. time.

occur as observed by Hounslow et al. (1988). The maximum allowable time step is set by the smallest grid spacing as:

$$\Delta t_{\max} = (L_{i+1} - L_i)_{\min}/G \tag{18}$$

Note that for parameter estimation studies, as the model growth parameters are adjusted, $\Delta t_{\max}$ will change. Also, for a batch crystallizer, G decreases during the run so that the allowable time step will increase with time. Computer CPU requirements can be minimized by increasing the step size during the simulation.

Simulations

Computer test studies

The parameter identification tests were performed as: (1) for a given set of kinetic parameters, the batch crystallizer model is used to generate a simulated data set consisting of a desupersaturation curve and final CSD for a seeded isothermal crystallization process; (2) the resulting measurement set is input to SimuSolv, and the nonlinear optimization is performed to recover the kinetic parameters. To balance computer run times and model accuracy, the size axis discretation used in the model is 150 increments from 4–1,400 μm with fixed ratio discretation ($r = 1.2042$) below 60 μm and fixed interval discretation ($\Delta\mathcal{L} = 10$ μm) above 60 μm. The 60-micron breakpoint features a smooth transition of class size along the axis as well as even distribution of overestimation error for each discretation scheme (the combined overestimation of the third moment for this discretation scheme is approximately 12%). The model includes the time-delayed formulation for nucleation (Appendix B).

The operating conditions were chosen to be similar to a typical pilot study—a seeded isothermal potash alum-water system in a 27-L vessel with initial supersaturation (S) of 4.7% (Rohani and Bourne, 1989). Crystallization is initiated by the addition of 5.0 g of seeds with a mean size of 325 μm (ranging from 275–375 μm) at time zero. For the four test cases, the supersaturation parameters (b/g) are maintained at 1.5/1.0, and the preexponential constants (k_g and k_b) are changed to span the entire range of growth and nucleation rates encountered in cooling, evaporative and precipitation processes as summarized by Garside and Shah (1980).

Table 1 summarizes the test conditions, while Figure 2 shows the range of growth and nucleation rates for the four test cases in comparison to the range of kinetics reported by Garside and Shah (1980). Figure 3 shows the profiles of uncounted crystals as computed by Eq. 15 vs. time. Table 1 shows a great deal of desupersaturation for runs 2 and 4 in contrast to runs 1 and 3 which were purposely halted with minimal desupersaturation. Intuitively, it is expected that runs 2 and 4 are more suitable for parameter identification. In fact, the results of this work show the opposite to be true: the data set for runs 1 and 3 contains more information as measured by the lower percentage of uncounted crystals (Figure 3) and is consequently easiest to identify.

Parameter identification definition

For each of the four test cases, SimuSolv is asked to identify four parameters k_g, k_b, b, and g. Table 2 lists the initial guess, as well as the upper and lower bounds, provided for the study.

For all tests, it is assumed that discrete measurements of the desupersaturation curve are available along with the percentage measurements of seed and product CSD. Using material balance calculations, the percentage CSD is converted to number of crystals in each size increment at $t = 0$ and $t = t_{\text{stop}}$. The measurement set (Eq. 8) is:

$$\begin{aligned} y = (&N_1, N_2, \quad \ldots, N_i)_{t=0}; \\ &(N_1, N_2, \quad \ldots, N_i)_{t=t\text{stop}}; \\ &(\Delta c^*_1, \Delta c^*_2, \quad \ldots, \Delta c^*_{t=t\text{stop}}) \end{aligned} \tag{19}$$

Table 1. Definition of Conditions for Computer Test Cases

Case	Kinetic Parameter				End of Run			
	$k_g \times 10^{-6}$	$k_b \times 10^{9}$	b	j,b	Time, s	wt. % N-cry	% Unc	S
1. Gmax—Bmin	20	1.08	1.5	1.0	400	4.5	5.8	4.6
2. Gmax—Bmax	20	1,080	1.5	1.0	600	96.5	15.2	0.1
3. Gmin—Bmin	2	1.08	1.5	1.0	5,000	49.0	8.4	4.4
4. Gmin—Bmax	2	1,080	1.5	1.0	2,400	96.9	34.1	1.0

Table 2. Definition of the Parameter Identification Problems

Case	Initial Guess (Upper Bound, Lower Bound)			
	$k_g \times 10^{-6}$	$k_b \times 10^{9}$	g	b
1	10 (60, 2.0)	0.108 (10^{3}, 10^{-2})	1.3 (1.7, 0.8)	1.7 (2.2, 1.2)
2	10 (60, 2.0)	108.0 (10^{4}, 10^{-2})	1.3 (1.7, 0.8)	1.7 (2.2, 1.2)
3	1 (6, 0.2)	0.108 (10^{3}, 10^{-2})	1.3 (1.7, 0.8)	1.7 (2.2, 1.2)
4	1 (6, 0.2)	108.0 (10^{4}, 10^{-2})	1.3 (1.7, 0.8)	1.7 (2.2, 1.2)

Here, the driving force vector Δc^* is defined by Eqs. 20 and 21. Note that for this work, all measurements are assumed to be free of noise.

Results and Discussion

Parameter identification

Transformation of Desupersaturation Data. Direct incorporation of concentration data (c or Δc) into the objective function as shown in Eq. 19 presented problems due to the very small change in the solution concentration. The concentration data in the measurement set were linearly transformed by:

$$\Delta c^* = a\Delta c - b \tag{20}$$

$$\Delta c = c - CE \tag{21}$$

where a is a constant related to the accuracy of the measurement, and b is a constant which magnifies the ratio of $\Delta c^*_{max}/\Delta c^*_{min}$. Since this transformation is linear, it does not effect error distribution assumptions and simply rescales and relocates the response function as discussed by Box and Draper (1987). For this study, the accuracy of the concentration data is assumed ± 0.000005 kg/kg, setting $a = 10{,}000$. Table 3 presents the transformed concentration data for case 3 using $a = 10{,}000$ and $b = 90$.

Deletion of Some Size Classes. Even after concentration data transformation, results were unsatisfactory in that SimuSolv only regressed the power law terms b and g, leaving k_g and k_b unchanged. Examination of the variance-covariance matrix at the known solution points indicated high variance and standard deviations for the k_g and k_b parameters. It was suspected that response variable correlation resulting from the material balance relationship between the desupersaturation data and the N vector was causing problems. The N vector in the measurement set was subsequently modified by deleting one or two size classes around the mean seed size to decouple the correlation. This modification improved deviations for k_g, but not for k_b. In addition, SimuSolv indicated that the Hessian matrix at the solution point is ill-conditioned, causing sensitivity problems when computing the search directions for parameters (Table 4).

Table 3. Concentration Data Transformation for Case 3

Time	c	Δc	Δc^*
0	0.22222	0.0100010	10.010
1,000	0.22218	0.0099596	9.596
2,000	0.22213	0.0099052	9.052
3,000	0.22203	0.0098145	8.145
4,000	0.22187	0.0096507	6.507
5,000	0.22159	0.0093651	3.651

Table 4. Variance-Covariance for Ill-Conditioned Hessian (Case 3)

	Variance-Covariance Matrix			
	k_g	g	k_b	b
k_g	9.181×10^{-12}			
g	4.631×10^{-17}	5.510×10^{-12}		
k_b	2.029×10^{-6}	-8.781×10^{-4}	1.219×10^{11}	
b	4.240×10^{-16}	-3.017×10^{-12}	21.58	4.364×10^{-9}

Kinetic Parameter Transformation. The sensitivity of the objective function to a parameter can be defined as:

$$\text{Sensitivity} = \frac{\partial \Phi}{\partial p} \tag{22}$$

For the nonlinear parameter transformation $p^* = g(p)$, the resulting new sensitivity becomes:

$$\frac{\partial \Phi}{\partial p^*} = \frac{dp}{dp^*}\frac{\partial \Phi}{\partial p} \tag{23}$$

The leading term may be regarded as a multiplier, and the transformation is chosen to produce a multiplier which avoids conditioning problems. The initial choice of a logarithmic transformation was replaced in favor of a tangent transformation which permitted the definition of a wider range for the multiplier. Defining the transformed parameters as:

$$k_g^* = \tan^{-1}(10^{g^*} \quad k_g) \tag{24a}$$

$$k_b^* = \tan^{-1}(10^{b^*} \quad k_b) \tag{24b}$$

results in the following sensitivities:

$$\frac{\partial \Phi}{\partial k_g^*} = 10^{-g^*}\, s^2(k_g^*)\frac{\partial \Phi}{\partial k_g} \tag{25a}$$

$$\frac{\partial \Phi}{\partial k_b^*} = 10^{-b^*}\, s^2(k_b^*)\frac{\partial \Phi}{\partial k_b} \tag{25b}$$

As defined in Eq. 19, the objective function derived from the N vector and desupersaturation curve depends highly on the process material balance. The optimization is most strongly influenced by growth kinetics and not very sensitive to nucleation. Referring to Eqs. 25a and 25b choosing $g^* > 0$ and $b^* < 0$ will have the effect of magnifying the sensitivity to the nucleation parameter in comparison to the growth parameter.

Model Eqs. 5 and 6 were rewritten in terms of k_g^* and k_b^*. Alternate values for g^* and b^* were used until the conditioning of the Hessian matrix improved and satisfactory parameter estimates obtained. It was found that $g^* = 7$, $b^* = -8$ were satisfactory for cases 1 and 3. Table 5 shows the resulting variance-covariance matrix for a well-behaved Hessian.

Problem Dependency of the Kinetic Parameter Transformation. The transformation defined by Eqs. 24a and 24b using $g^* = 7$ and $b^* = -8$ gave satisfactory results for test cases 1 and 3, but not for cases 2 and 4. By repeated trials and checking

Table 5. Variance-Covariance for Well Behaved Hessian (Case 3)

Transformation Used: $k_g^* = \tan^{-1}(k_g \cdot 10^7)$; $k_b^* = \tan^{-1}(k_b \cdot 10^{-8})$				
	k_g^*	g	k_b^*	b
k_g^*	2.877×10^{-12}			
g	9.824×10^{-12}	4.046×10^{-11}		
k_b^*	-6.925×10^{-12}	-2.970×10^{-11}	2.911×10^{-11}	
b	-1.454×10^{-11}	-6.899×10^{-11}	6.644×10^{-11}	1.648×10^{-9}

the conditioning of the variance-covariance matrix, satisfactory results are found for $g^* = 7$, $b^* = -8$ for case 2 and $g^* = 6$, $b^* = -10$ for case 4. Table 6 summarizes the best results and the values for b^* and g^* used.

Based on these findings, qualitative guide lines for selecting g^* and b^* based on manipulation of the objective function sensitivity multiplier can be proposed. Considering first the selection of b^*, note that for cases 2 and 4, the total percentage N-crystals is highest as is the percentage uncounted crystals (Table 1).Choosing b^* more negative in comparison to runs 1 and 3 increases the sensitivity to k_b (per Eq. 25b) and improves results. In a similar manner, cases 2 and 4 exhibit the highest desupersaturation. Considering the selection of g^*, choosing g^* less positive in comparison to runs 1 and 3 increases the sensitivity to k_g. Note that run 2 has the highest desupersaturation and the least positive g^*.

Further improvements for cases 2 and 4 may be obtained by modifying the experimental conditions to reduce the percent of uncounted crystals. For case 2, if the initial supersaturation is changed from 4.7 to 0.3, the percent uncounted changes from 15.2% to 9.3%. For case 4, if the seed quantity is changed from 0.005 kg to 0.05 kg, the percent uncounted changes from 34% to 27%. The improved parameters in Table 7 were obtained under these conditions. Case 4 which initially had the highest percentage of crystals below 4 micron shows the greatest improvement.

Importance of delayed nucleation model

As observed in Table 1, for runs 2 and 4 with the highest nucleation rates, the percent of uncounted crystals (Eq. 15) is highest. For these cases, the time delay formulation for nucleation is most important. Figure 4 compares the desupersaturation curves with and without the delay formulation for case 2. At 50% of equilibrium, ignoring the time required for crystals to grow from cluster to 4 micron will overpredict desupersaturation by approximately 20%.

Conclusion

Working with computer-generated data, it is shown that values for nucleation and growth kinetic parameters may be successfully identified for a wide range of process conditions using SimuSolv. In all cases, however, accurate parameter identification requires the use of nonlinear parameter transformations. This finding parallels those of Ratkosky (1985) on the kinetics of solid-phase catalytic reactions.

It is also shown that the proper choice for transformation is problem-dependent, becoming more sensitive as nucleation rates increase and the percentage of crystals below the measurable range increases. For these processes, the information content of the CSD measurement is relatively incomplete, thereby magnifying nonlinear behavior. As shown in Tables 6 and 7, experimentation with transformations as well as modification of experimental conditions to minimize fines is recommended to improve results.

Table 6. Best Results Using Parameter Transformation

Case	Identified Parameter				Transformation	
	$k_g \times 10^{-6}$	$k_b \times 10^9$	b	g	b^*	g^*
1. *G*max-*B*min	20	2.30	1.66	1.00	−8	7
2. *G*max-*B*max	12	3,200	1.65	0.80	−10	5
3. *G*min-*B*min	3.2	1.50	1.57	1.10	−8	7
4. *G*min-*B*max	2.4	130	1.68	1.11	−10	6

Table 7. Best Results After Modifying Experiment

Case	Identified Parameter				Modification
	$k_g \times 10^{-6}$	$k_b \times 10^9$	b	g	
2. *G*max-*B*max	12	2,600	1.50	0.82	Decrease initial S
4. *G*min-*B*max	1.1	830	1.60	1.00	Increase seeds

Acknowledgment

The authors wish to acknowledge the support of Dan Green (E. I. DuPont de Nemours and Company, Inc.), Tom Broadhurst (Esso Petroleum Canada) and Bob Blanks (Amoco Chemical Co.) as well as the critical review of Pat McCroskey (Dow Chemical Co.), and Allan Myerson (Polytechnic University).

Notation

b = nucleation order
B_0 = nucleation rate, No. /(m^3·s)
c = concentration of solution, kg/kg H_2O
CE = equilibrium concentration of solution, kg/kg H_2O
G = linear growth rate, m/s
g = growth order
j = magma density order
k_b = kinetic coefficient for nucleation
k_g = kinetic coefficient for growth
L = size of crystals, m
$\bar{L}$ = number mean size, m
$\bar{L}_{j,k}$ = $(m_j/m_k)^{1/(j-k)}$, m
m_j = jth crystal moment

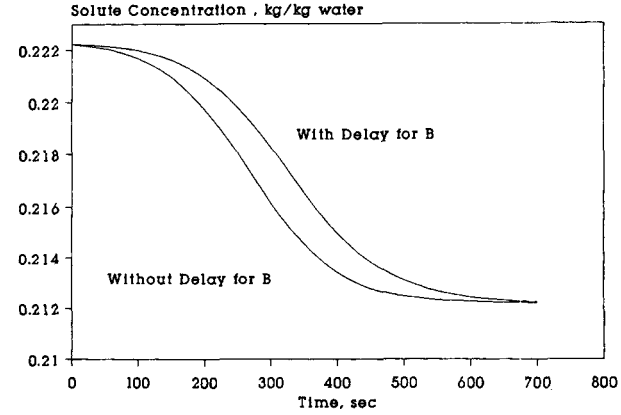

Figure 4. Effect of time-delayed nucleation on desupersaturation.

MT = magma density kg/m^3 suspension
N_i = number of particles in interval i, No. /m^3
p = parameter vector
r = geometric ratio
S = relative supersaturation, $[(c-CE)/CE]\times 100$
t = time, s
T = temperature, °C
y = measurement vector

Subscript and Superscript

i = discrete crystal-size index
* = transformed variable
$\overline{\ }$ = model variable

Literature Cited

Bates, D. M., and D. G. Watts, *Nonlinear Regression Analysis & Its Applications*, Wiley, New York (1988).

Bates, D. M., and D. G. Watts, "Parameter Transformations for Improved Approximate Confidence Regions in Nonlinear Least Squares," *Annals of Statistics*, **9**(6), 1152 (1981).

Box, G. E. P., and W. J. Hill, "Discrimination Among Mechanistic Models," *Technometrics*, **9**, 57 (1967).

Box, G. E. P., and N. R. Draper, *Empirical Model-Building And Response Surfaces*, p. 280, Wiley, New York (1987).

Buyevich, Y. A., V. V. Mansurov, and I. A. Natalukha, "Instability and Unsteady Processes of the Bulk Continuous Crystallization: 1. Linear Stability Analysis," *Chem. Eng. Sci.*, **46**(10), 2573 (1991).

Chen, N. H., and R. Aris, "Determination of Arrhenius Constants by Linear and Nonlinear Fitting," *AIChE J.*, **38**(4), 626 (1992).

deWolf, S., J. Jager, B. Visser, H. J. M. Kramer, and O. H. Bosgra, "Derivation of State Space Models of Crystallizers," *ACS Symp. Ser.*, **438**, 144 (1990).

Eaton, J. W., and J. B. Rawlings, "Feedback Control of Chemical Processes Using On-Line Optimization Techniques," *Comp. & Chem. Eng.*, **14**(4/5), 469 (1990).

Edgar, T. F., and G. T. Wright, "Nonlinear Model Predictive Control of a Fixed Bed Water Gas Shift Reactor: An Experimental Study," AIChE Meeting, Miami (1992).

Garside, J., and M. B. Shah, "Crystallization Kinetics from MSMPR Crystallizers," *Ind. Eng. Chem. Proc. Des. Dev.*, **19**, 509 (1980).

Hostomsky, J., and A. G. Jones, "Calcium Carbonate Crystallization, Agglomeration and Form During Continuous Precipitation From Solution," *J. Phys. D: Appl. Phys.*, **24**, 165 (1991).

Hounslow, M. J., "A Discretized Population Balance for Continuous Systems at Steady State," *AIChE J.*, **36**(1), 106 (1990).

Hounslow, M. J., R. L. Ryall, and V. R. Marshall, "A Discretized Population Balance for Nucleation, Growth, and Aggregation," *AIChE J.*, **34**(11), 1821 (1988).

Jager, J., H. J. M. Kramer, B. Scarlett, and E. J. deJong, "Effect of Scale of Operation on CSD Dynamics in Evaporative Crystallizers," *AIChE J.*, **37**(2), 182 (1991).

Kramer, H. J. M., S. deWolf, and J. Jager, "Simulation of the Dynamic Behavior of Continuous Crystallizers," *ACS Symp. Ser.*, **438**, 159 (1990).

Marchal, P., R. David, J. P. Klein, and J. Villermaux, "Crystallization and Precipitation Engineering I: An Efficient Method for Solving Population Balance in Crystallization With Agglomeration," *Chem. Eng. Sci.*, **43**(1), 59 (1988).

Qui, Y., and A. C. Rasmuson, "Nucleation and Growth of Succinic Acid in a Batch Cooling Crystallizer," *AIChE J.*, **37**(9), 1293 (1991).

Ratkowsky, D. A., "A Statistically Suitable General Formulation for Modelling Catalytic Chemical Reactions," *Chem. Eng. Sci.*, **40**(9), 1623 (1985).

Ratkowsky, D. A., *Nonlinear Regression Modeling A Unified Practical Approach*, Marcel Dekker, New York (1983).

Randolph, A. D., and M. A. Larson, *Theory of Particulate Process*, 2nd ed., Academic Press, New York (1988).

Rohani, S., and J. R. Bourne, "Self-Tuning Control of Crystal Size Distribution in a Batch Crystallizer," AIChE Meeting, San Francicso (1989).

Stewart, W. E., M. Caracotsios, and J. P. Sorensen, "Parameter Estimation From Multiresponse Data," *AIChE J.*, **38**(5), 641 (1992).

Steiner, E. C., T. D. Rey, and P. S. McCroskey, *SimuSolv Reference Guide*, Dow Chemical Co. (1990).

Tavare, N. S., and J. Garside, "Simultaneous Estimation of Crystal Nucleation and Growth Kinetics from Batch Experiments," *Chem. Eng. Res. Des.*, **64**, 109 (1986).

Witkowski, W. R., S. M. Miller, and J. B. Rawlings, "Robust Kinetic Parameter Estimation of Crystallization Processes," AIChE Meeting, San Francisco (1989).

Appendix A: Overestimation Factor for Fixed Interval Discretation

Summing over all discrete sizes according to:

$$m_j=\sum_i (\overline{L_i^j}N_i) \tag{A1}$$

$$\overline{L_i^j}=\frac{1}{j+1}\frac{\mathcal{L}_{i+1}{}^{j+1}-\mathcal{L}_i^{j+1}}{\Delta\mathcal{L}} \tag{A2}$$

$$m_j=\sum_i\left(\frac{1}{j+1}\frac{\mathcal{L}_{i+1}{}^{j+1}-\mathcal{L}_i^{j+1}}{\Delta\mathcal{L}}\right)N_i \tag{A3}$$

Taking the time derivatives,

$$\frac{dm_j}{dt}=\sum_i\left(\frac{1}{j+1}\frac{\mathcal{L}_{i+1}{}^{j+1}-\mathcal{L}_i^{j+1}}{\Delta\mathcal{L}}\right)\frac{dN_i}{dt} \tag{A4}$$

where, for fixed intervals, dN_i/dt is,

$$\frac{dN_i}{dt}=G\left(\frac{N_{i-1}-N_i}{\Delta\mathcal{L}}\right) \tag{A5}$$

Inserting dN_i/dt for Eq. A4 and rearranging,

$$\frac{dm_j}{dt}=\frac{1}{j+1}\frac{G}{\Delta\mathcal{L}}\sum_i\left(\frac{\mathcal{L}_{i+1}{}^{j+1}-\mathcal{L}_i^{j+1}}{\Delta\mathcal{L}}(N_{i-1}-N_i)\right) \tag{A6}$$

Further arrangement of Eq. A6 results in the following:

$$\frac{dm_j}{dt}=\frac{1}{j+1}\frac{G}{\Delta\mathcal{L}}\left\{\sum_i\left(\frac{\mathcal{L}_{i+1}{}^{j+1}-\mathcal{L}_i^{j+1}}{\Delta\mathcal{L}}N_{i-1}\right)-\sum_i\left(\frac{\mathcal{L}_{i+1}{}^{j+1}-\mathcal{L}_i^{j+1}}{\Delta\mathcal{L}}N_i\right)\right\} \tag{A7}$$

Expanding the numerator of the first summation term of Eq. A7:

$$\begin{aligned}&=(\mathcal{L}_i+\Delta\mathcal{L})^{j+1}-(\mathcal{L}_{i-1}+\Delta\mathcal{L})^{j+1}\\&=\left[\mathcal{L}_i^{j+1}+\binom{j+1}{1}\mathcal{L}_i^j\Delta\mathcal{L}+\binom{j+1}{2}\mathcal{L}_i^{j-1}\Delta\mathcal{L}^2+\cdots\cdots+\Delta\mathcal{L}^{j+1}\right]\\&-\left[\mathcal{L}_{i-1}{}^{j+1}+\binom{j+1}{1}\mathcal{L}_{i-1}{}^j\Delta\mathcal{L}+\binom{j+1}{2}\mathcal{L}_{i-1}{}^{j-1}\Delta\mathcal{L}^2-\cdots\cdots-\Delta\mathcal{L}^{j+1}\right]\end{aligned} \tag{A8}$$

Collecting terms:

$$=(\mathcal{L}_i^{j+1}-\mathcal{L}_{i-1}^{j+1})+\binom{j+1}{1}\Delta\mathcal{L}(\mathcal{L}_i^{j}-\mathcal{L}_{i-1}^{j})+\binom{j+1}{2}$$

$$\Delta\mathcal{L}^2(\mathcal{L}_i^{j-1}-\mathcal{L}_{i-1}^{j-1})+\ldots.\ \mathcal{L}_{i+1}^{j+1}-\mathcal{L}_i^{j+1}=\sum_{k=0}^{j}\binom{j+1}{k}$$

$$\Delta\mathcal{L}^k(\mathcal{L}_i^{j+1-k}-\mathcal{L}_{i-1}^{j+1-k}) \quad \text{(A9)}$$

Substituting Eq. A9 into the first summation term in Eq. A7,

$$\sum_i\left(\frac{\mathcal{L}_{i+1}^{j+1}-\mathcal{L}_i^{j+1}}{\Delta\mathcal{L}}N_{i-1}\right)=\sum_i\left\{\frac{N_{i-1}}{\Delta\mathcal{L}}\left[\sum_{k=0}^{j}\binom{j+1}{k}\right.\right.$$

$$\left.\left.\Delta\mathcal{L}^k(\mathcal{L}_i^{j+1-k}-\mathcal{L}_{i-1}^{j+1-k})\right]\right\}$$

$$=\sum_{k=0}^{j}\left\{\binom{j+1}{k}\Delta\mathcal{L}^k\left[\sum_i\frac{\mathcal{L}_i^{j+1-k}-\mathcal{L}_{i-1}^{j+1-k}}{\Delta\mathcal{L}}N_{i-1}\right]\right\}$$

$$=\sum_{k=0}^{j}\binom{j+1}{k}\Delta\mathcal{L}^k(j+1-k)m_{j-k} \quad \text{(A10)}$$

Using Eq. A3, the second summation term in Eq. A7 is simply:

$$\sum_i\left(\frac{\mathcal{L}_{i+1}^{j+1}-\mathcal{L}_i^{j+1}}{\Delta\mathcal{L}}N_i\right)=(j+1)m_j \quad \text{(A11)}$$

Now, inserting Eqs. A10 and A11, Eq. A7 becomes:

$$\frac{dm_j}{dt}=\frac{1}{j+1}\frac{G}{\Delta\mathcal{L}}\left\{\sum_{k=0}^{j}\binom{j+1}{k}\Delta\mathcal{L}^k(j+1-k)m_{j-k}-(j+1)m_j\right\}$$

$$=\frac{G}{j+1}\sum_{k=1}^{j}\binom{j+1}{k}\Delta\mathcal{L}^{k-1}(j+1-k)m_{j-k} \quad \text{(A12)}$$

Rearranging,

$$\frac{dm_j}{dt}=jGm_{j-1}\left[\frac{1}{j(j+1)}\sum_{k=1}^{j}\binom{j+1}{k}\Delta\mathcal{L}^{k-1}\right.$$

$$\left.\times(j+1-k)\frac{m_{j-k}}{m_{j-1}}\right] \quad \text{(A13)}$$

The third moment is:

$$\frac{dm_3}{dt}=3Gm_2\left(1+\Delta\mathcal{L}\frac{m_1}{m_2}+\frac{\Delta\mathcal{L}^2}{3}\frac{m_0}{m_2}\right)$$

$$=3Gm_2\left(1+\frac{\Delta\mathcal{L}}{\overline{L}_{2,1}}+\frac{1}{3}\frac{\Delta\mathcal{L}^2}{\overline{L}_{2,0}^2}\right) \quad \text{(A14)}$$

Appendix B: Formulation for Time-Delayed Nucleation

Assume that all nucleated crystals are born at zero size. Crystals that have not grown to the first size increment L_1 are assumed to reside in a queue. The length of the queue is defined along the size axis as L_1. At each integration step, a packet of crystals BPACK is borne.

Consider integration time t. The number of particles born at zero size is computed according to Eq. 6:

$$(B\text{PACK})_t=(B_0)_t=k_b\Delta c^bMT^j \quad \text{(B1)}$$

The linear growth rate at time t is computed according to Eq. 5:

$$(G)_t=k_g\Delta c^g \quad \text{(B2)}$$

At the next integration step $t+\Delta t$, the distance through the queue traveled by packet $B\text{PACK}_t$ is defined as $L\text{PACK}_t$ given by:

$$(L\text{PACK})_t=(G)_t\Delta t \quad \text{(B3)}$$

For the second integration step, the distance through the queue traveled by packet $B\text{PACK}_t$ is given by:

$$(L\text{PACK})_t=(G)_t\Delta t+(G)_{t+\Delta t}\Delta t \quad \text{(B4)}$$

At any time increment, individual packets exit the queue if $(L\text{PACK})_t>L_1$.

$$\text{If } [(L\text{PACK})_t>L_1]B\text{EXIT}_1=(L\text{PACK})_t \quad \text{(B5)}$$

At each time step, the particles appearing in the first discrete size increment of the model (B_1) is computed by summing over all packets:

$$B_1=\Sigma\ B\text{EXIT}_i \quad \text{(B6)}$$

Manuscript received Feb. 11, 1993, and revision received Aug. 11, 1993.